

EnhanceGraph: A Continuously Enhanced Graph-based Index for High-dimensional Approximate Nearest Neighbor Search

Xiaoyao Zhong^{1,2}, Jiabao Jin², Peng Cheng¹, Mingyu Yang^{2,3}, Haoyang Li⁴,
Zhitao Shen², Heng Tao Shen¹, Jingkuan Song¹

¹Tongji University, Shanghai, China; ²Ant Group, Shanghai, China; ³HKUST (GZ), Guangzhou, China; ⁴PolyU, Hong Kong SAR, China
{zhongxiaoyao.zxy, jinjiabao.jjb, yangming.ymy, zhitao.szt}@antgroup.com; cspcheng@tongji.edu.cn;
haoyang-comp.li@polyu.edu.hk; shenhengtao@hotmail.com; jingkuan.song@gmail.com

Abstract—Recently, Approximate Nearest Neighbor Search in high-dimensional vector spaces has garnered considerable attention due to the rapid advancement of deep learning techniques. We observed that a substantial amount of search and construction logs are generated throughout the lifespan of a graph-based index. However, these two types of valuable logs are not fully exploited due to the static nature of existing indexes. We present the EnhanceGraph framework, which integrates two types of logs into a novel structure called a conjugate graph. The conjugate graph is then used to improve search quality. Through theoretical analyses and observations of the limitations of graph-based indexes, we propose several optimization methods. For the search logs, the conjugate graph stores the edges from local optima to global optima to enhance routing to the nearest neighbor. For the construction logs, the conjugate graph stores the pruned edges from the proximity graph to enhance retrieving of k nearest neighbors. Our experimental results on several public and real-world industrial datasets show that EnhanceGraph significantly improves search accuracy with the greatest improvement on recall from 41.74% to 93.42%, but does not sacrifice search efficiency. In addition, our EnhanceGraph algorithm has been integrated into Ant Group’s open-source vector library, VSAG.

Index Terms—Approximate Nearest Neighbor Search, Graph-based Index

I. INTRODUCTION

With the rapid development of deep learning in various fields, it has become a common trend to use vectors for representing entities. Many applications now require finding the most similar points of a given query point in a large database, known as nearest neighbor search problem, which is widely used in scenarios such as facial recognition [1], recommendation systems [2], and information retrieval [3]. Due to the “Curse of Dimensionality” [4], [5], finding accurate nearest neighbors in high-dimensional data sets is often computationally intensive. Then, Approximate Nearest Neighbor Search (ANNS) has gained significant attention as it can retrieve the nearest neighbors with acceptable deviations under limited space and time constraints.

There have been many ANNS methods recently, such as graph-based methods [6], [7], [8], [9], tree-based methods [10], [11], [12], [3] and hashing-based methods [13], [14], [15]. Numerous studies [16], [17] demonstrate that graph-based algorithms show superior search performance. Graph-based

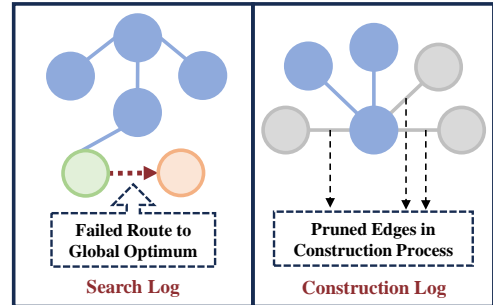


Fig. 1: Example of Search and Construction Log. We use the search log to add edges that can route from local optimum (searched approximate nearest neighbor) to the global optimum (exact nearest neighbor), enhancing recall of the nearest neighbor. The construction log maintains pruned nearest neighbors to further improve recall of nearest neighbors.

methods first construct a *proximity graph*, where each node represents a base data point in the database, and the edges connect similar points. To find the nearest neighbors of a query point, they usually pick a start point on the graph index, then greedily traverse to the target nearest point to the query point. In addition, k -Nearest Neighbors (k -NNs) Graph [18], [19] is used to maintain the connections of similar points, where a node u is connected to a node v with a directed edge if v is one of the k -NNs of u .

To reduce the space usage and search efficiency, recent studies apply Relative Neighborhood Graph (RNG) [20], [21], [6], [9] and Monotonic Relative Neighborhood Graph (MRNG) [7], [22], [23], [8] edge pruning strategies to remove edges from the k -NNs Graph on building the proximity graph index. However, due to the pruning of edges, the queries on the proximity graph may return results with some deviations or even fail to retrieve the nearest neighbors. In addition, the graph-based indexes will stay static after construction. From our observations on facial recognition services, many users experience repeated failures to be recognized using HNSW [9]. In other words, the graph-based indexes built with the existing methods suffer from “*flaws*” that prevent them from accurately retrieving the nearest neighbors of the queried points. *How*

to fix the flaws such that the accuracy of the graph-based indexes can be improved with acceptable space costs is a long-standing problem for the ANNS topic. According to our observations, the search log and construction log have not been well used to refine the graph-based indexes in the existing studies.

Specifically, the *search log* is not utilized due to the static graph structure. The graph will remain *static* once all dynamic operations (e.g., insert or delete) are completed. If a historical search query cannot find the nearest neighbor on the existing static index, then other similar future queries will also fail to find it. However, a vast amount of historical query data exists in many industrial applications. Through analysis of a large amount of data, we have observed that similar query points tend to converge to the same local optimum (i.e. the nearest neighbor in search result). It allows us to leverage the search log from existing historical queries or generated queries, providing an opportunity for refining of the graph-based index.

In addition, a significant amount of *construction log* is not effectively utilized for index optimization. During the construction process, each base point in the database is searched for its k -NNs. With edge pruning strategies, not all k -NNs are included in proximity graph. However, they have the potential to be found as k -NNs. The existing graph-based methods can hardly localize the accurate k -NNs, which is mainly due to the inability to distinguish between edges that contribute to the search process. Simply removing edges directly increases the uncertainty of locating the k -NNs.

Our Idea:

In the existing studies, the graph-based indexes typically remain static once built. We find that the search log can be used to detect flaws in the graph structure, and the construction log can be used to supplement the missing k -NNs for the proximity graph. In this paper, we propose a framework, namely *EnhanceGraph*, to utilize search and construction logs for dynamic enhancement of graphs, enabling a significant improvement on query accuracy with an acceptable increase in space costs.

Specifically, as shown in Figure 1, in *EnhanceGraph*, we use the conjugate graph to store the pruned edges of proximity graph that are valuable for the search process. When constructing the graph index, we first add the pruned edges from proximity graph to the conjugate graph. Then, we heuristically generate k training queries for each base data point on the proximity graph, which can be used to detect flaws in the graph structure (i.e., local optima). Using the generated queries along with historical search log, we add the missing edges that can route local optima to global optimum (i.e., the nearest neighbor) in the conjugate graph such that the flaws can be fixed. For new queries, we take a small step in the conjugate graph to route from local optima to global optima. Thus, we can guarantee that the historically failed queries will not converge to a local optimum again. Once we guarantee finding the global optimum in high probability, the conjugate graph can further return other nearest neighbors accurately

efficiently. Our *EnhanceGraph* has been integrated into Ant Group’s open-source vector library, VSAG¹.

To summarize, we make the following contributions:

- We introduce the *EnhanceGraph* framework, which is the first to leverage the search and construction logs to continuously enhance the search process in Section III.
- We discuss how to address flaws on graph-based indexes and the optimization opportunities based on observations and theoretical analysis in Section IV.
- We propose two optimizations based on the conjugate graph to improve accuracy in search process in Section V.
- We conduct extensive experiments on both public datasets and an anonymous industrial dataset in Section VI.

II. PRELIMINARY

Definition 1. (k -NNs Search) Given a dataset D and a query point x_q , along with a positive integer k , the k -NNs search aims to find a set $NN_k(x_q)$ containing k points, such that for all $x_r \in NN_k(x_q)$ and all $x_b \in D \setminus NN_k(x_q)$, the condition $dis(x_r, x_q) \leq dis(x_b, x_q)$ holds. Here, $dis(x_1, x_2)$ denotes the distance between two points in a specific metric space, such as Euclidean or Cosine distance.

However, due to the large dimension of the data, it’s difficult to find accurate k -NNs. Recent studies [24], [25], [15] focus on Approximate Nearest Neighbors Search (ANNS), which only requires searching approximate k -NNs. For ANNS, the evaluation of search results is based on the recall rate. Let $NN_k(x_q)$ represent the accurate set of k -NNs, and $ANN_k(x_q)$ represent the approximate set of k -NNs. The recall rate is then defined as $Recall@k = \frac{|ANN_k(x_q) \cap NN_k(x_q)|}{k}$. The nearest neighbor of the query point x_q within the dataset D is denoted as x_g , where $x_g = \arg \min_{x_b \in D} dis(x_b, x_q)$.

Definition 2. (Proximity Graph) Given a dataset D , the proximity graph can be denoted as $G = (V, E)$, where each nodes $v \in V$ represents a base point $x_b \in D$.

In general, each node in a proximity graph is connected to points that are close to it.

III. ENHANCEGRAPH FRAMEWORK

A. Search on Proximity Graph

Algorithm 1 illustrates the greedy search [23], [7], [9] process of finding the approximate k -NNs on a proximity graph. To begin the search, we initialize a maximum heap of size L as the candidate set (Line 1). In most cases, k is fixed, whereas users can adjust the heap size L to balance accuracy and efficiency. The heap is ordered based on distance to facilitate the quick retrieval of the $k \leq L$ nearest points. Next, we initiate the greedy search from the given initial nodes (Line 2) and iteratively explore each point c in the candidate set C that has not yet been expanded, i.e., whose neighbors have not been visited (Lines 3-5). If the distance of some neighbors is less than that of the node with the largest

¹<https://github.com/alipay/vsag>

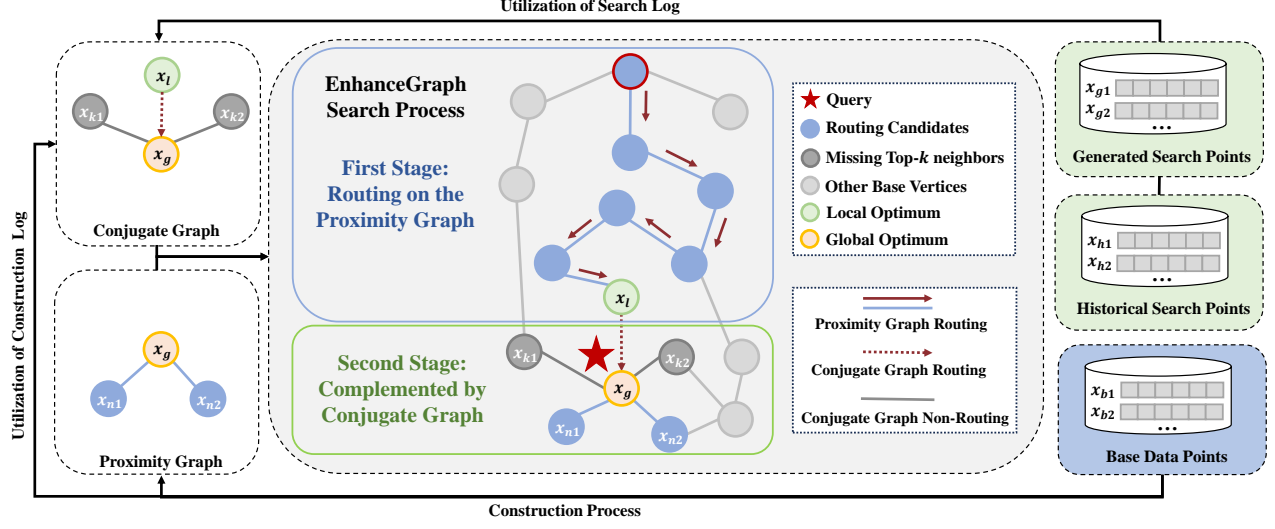


Fig. 3: A Pipeline of the EnhanceGraph Framework. We utilize both search and construction log to construct a conjugate graph. A query is initially routed through the proximity graph. Subsequently, both routing and non-routing edges in the conjugate graph are employed to navigate from the local optimum in the proximity graph to the global optimum and to complement the missing k -NNs.

certain failed queries consistently failing without any opportunity for correction, a problem that is difficult to identify in generalized methods. On the contrary, in our framework, we adopt a data-driven approach using the *search log*. If we have the historical query logs, we can identify the local optimum that most queries converge to. A local optimum arises due to the absence of routing edges from the local optimum to the global optimum. If many similar queries all lead to the same local optimum, we can guarantee that all those queries can reach their global optimum by adding edges from the local optimum to the global optimum. Therefore, the search log can be utilized to continuously optimize the graph-based indexes.

The Utilization of Construction Log. Determining which edges are non-routing is relatively easier. To improve Recall@ k is to increase the overlap between the graph-based indexes and the full k -NNs graph (i.e., k -NNs graph contains all non-routing edges). However, the existing edge pruning strategies remove many close neighbors to improve the search speed and decrease the space cost. As a consequence, non-routing edges are inevitably absent. Therefore, the key issue is how to construct an approximate k -NNs graph that retains more important non-routing edges and utilizes them in the specific search phase. We can leverage the *construction log* to help us achieve this. During the graph construction process, each base point is repeatedly searched on the graph for its k -NNs. However, the search results are only used for pruning. Instead, we can store the pruned edges of each base point into a conjugate graph to complement the proximity graph.

Framework. In this paper, we propose a framework, namely EnhanceGraph, to utilize both construction and search log to continuously optimize the graph-based index. As shown in

Algorithm 2: Greedy Search with Conjugate Graph

Input: proximity graph G , conjugate graph G' , initial nodes I , query point x_q , search parameters L, k
Output: Approximate k -NNs of x_q in G , visited nodes V

- 1 $R, V \leftarrow \text{GreedySearch}(G, I, x_q, L, k)$
- 2 $x_l \leftarrow$ the nearest point of x_q in R
- 3 $x_g \leftarrow$ the nearest point of x_q in $G'[x_l] \cup \{x_l\}$
- 4 $V' \leftarrow V \cup G'[x_g] \cup \{x_g\}$
- 5 $R' \leftarrow$ top- k nearest points of x_q in $G'[x_g] \cup \{x_g\} \cup R$
- 6 **return** Approximate k -NNs R' , visited nodes V'

Fig. 3, we first use the construction log to build the proximity graph and conjugate graph. Specifically, each base point is searched for its k -NNs during the construction process. Then, we insert pruned edges into the conjugate graph and insert the remaining edges into proximity graph. We use the search log from both generated and historical queries to further improve the conjugate graph. Specifically, we connect the local optima with their corresponding global optima in the search log. Then, the proximity graph is used for searching a preliminary result, and the conjugate graph is used as enhancement for the result.

As shown in Algorithm 2, we utilize the conjugate graph to enhance the greedy search process. First, we search the proximity graph for preliminary nearest neighbors and the local optima (line 1-2). Next, we utilize the connections of those local-global optima pairs that are stored in the conjugate graph based on search log. It is possible to retrieve the global optimum from the neighbors of $G'[x_l]$ (line 3). Once we reach the global optimum of the query point, we use its neighbors

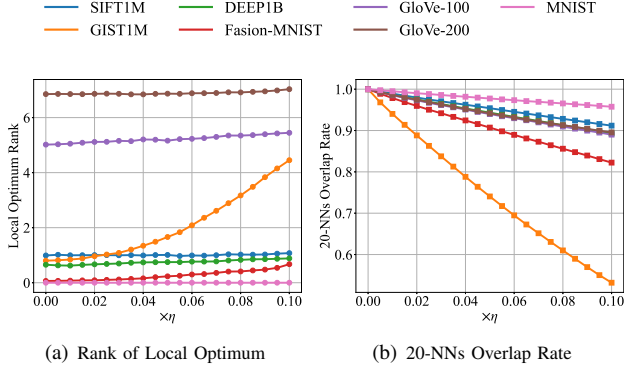


Fig. 4: Rank of Local Optimum and 20-NNs Overlap Rate (Observation 1 and Observation 2). “Rank” means the rank of local optimum in the nearest neighbors of global optimum, i.e., the rank of nearest neighbor of global optimum is 1.

$G'[x_g]$ in the conjugate graph as the complement of the k -NNs (line 4-5).

IV. OPPORTUNITIES OF ENHANCEMENT

A. Observations and Opportunities

In real-world applications (e.g., facial recognition), there are users who fail many times to search their accurate k -NNs (e.g., their own facial images). Existing indexes are trapped in these situations due to their *static nature*, which leads to subsequent queries repeating the same mistakes. *Note that, here we say the existing graph indexes have static nature referring to that their graph edges are forbidden to be changed after construction.* However, the abundant search log has not been effectively utilized to detect graph flaws and refine its structure. We heuristically guide how to utilize the search log through several observations and opportunities.

Theorem IV.1. *Given the query point x_q , it's accurate k -NNs set $NN_k(x_q)$ and approximate k -NNs set $ANN_k(x_q)$, we assume x_l is the local optimum of the approximate k -NNs of query point x_q . If $Recall@k > 0$, we have $x_l \in NN_k(x_q)$.*

Proof. We prove it by contradiction. Assume that there's a point $x_l \notin NN_k(x_q)$ that is the local optimum. Given that $Recall@k > 0$, there must be another point $x'_l \in ANN_k(x_q)$ in the search result that satisfies $x'_l \in NN_k(x_q)$. Since $x'_l \in NN_k(x_q)$, we have $dis(x'_l, x_q) < dis(x, x_q), \forall x \notin NN_k(x_q)$, where x is another base point. Since $x_l \notin NN_k(x_q)$, we have $dis(x'_l, x_q) < dis(x_l, x_q)$. According to Definition 3, we have x_l is not the local optimum, contradicting our initial assumption.

Opportunity 1: Local optimum is likely the one of k -NNs of the global optimum. Any query point x_q is in the neighborhood of its nearest neighbor x_g . Since they are both surrounded by the neighbors of x_g , we have another heuristic: *the neighbors of query point x_q and the neighbors of its nearest neighbor x_g are highly overlapping.* According to the theorem IV.1, as long as the $Recall@k > 0$, the local optimum x_l of the search process must be in the accurate k -NNs of the

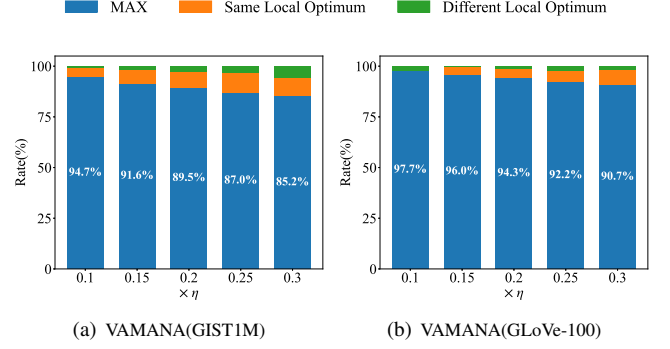


Fig. 5: Same Local Optimum Rate of Similar Point (Observation 3).

query point x_q . Combining the heuristic and theorem, we can infer that $x_l \in NN_k(x_g)$ with high probability.

Observation 1. Figure 4(a) shows the trend of ranks, where a smaller rank indicates local optimum is closer to the global optimum. We generate the test queries by calculating the mean η of each dimension of base vectors and adding positive noise (e.g., $0.06 \times \eta$) to them. Next, we conduct searches on the GIST1M and GLoVe-100 datasets using the VAMANA [23] index. We find that a significant proportion of the searched local optima are neighbors to the global optimum, and they often constitute the closer neighbors (i.e., rank less than 7).

Observation 2. Figure 4(b) shows the trend of the overlap rate, which represents the proportion of identical neighbors in the 20-NNs of both the query and the base points. In most cases, there is a considerable portion (i.e., greater than 60%) of overlap. Besides, the overlap rate decreases as the similarity of the generated points decreases (i.e., moves to the right of the x-axis).

Opportunity 2: Similar points may converge to the same local optimum. Most graph-based indexes have a fixed starting point for searching to ensure a Monotonic Decrease Path [7] from that point to any base point [7], [22], [8]. It means that similar points may have similar search paths and thus converge to the same local optimum.

Observation 3. As shown in Figure 5, we generate queries by adding noise sampled from a uniform distribution (e.g. $U(-0.2 \times \eta, 0.2 \times \eta)$). The blue and orange bars indicate the queries converged to some same local optima. The blue bar indicates the percentage of the most queries converged to one same local optimum. For example, assume we have 10 queries converging to base points with IDs (1, 1, 1, 1, 1, 1, 2, 2, 3). There are two local optima (i.e., IDs 1 and 2) that have at least two queries converging to them. The “MAX” local optimum ID is 1, with a corresponding percentage of 7/9, shown in the blue bar. The percentage of 2/9 for the other local optimum (i.e., ID 2) is displayed in the orange bar and the percentage of 1/9 for the single local optimum (i.e., ID 3) is displayed in the green bar. We find that a large number of similar points (up to 97.7%) converge to the same local optimum on two datasets.

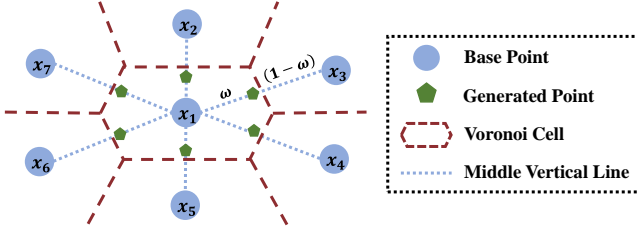


Fig. 6: Example of Generated Points in Voronoi Diagram.

Discussion. Together with theoretical analyses and data analyses, we conclude that the local optima of similar points tends to be the k -NNs of corresponding base points. Since the queries with the same global optimum are similar, we can utilize historical search logs to enhance the performance of online queries to avoid future repeating failures of them. Regrettably, the recall rate requirement for real-world applications (e.g., facial recognition) is usually very high. Consequently, historical search logs may be inadequate, as they only reveal a limited number of local optima. Therefore, we propose an efficient method that generates queries to identify flaws in the graph index (i.e., potential local optima) and collects self-generated search logs. Due to space limitation, please refer to Appendix IV-B for details on the self-generated search logs.

B. Self-Generated Search Log

In addition to utilizing historical search logs, we can also generate queries using heuristic methods. The search log from these generated queries can also continuously optimize the graph through identifying potential flaws. Thus, we first investigate which types of queries are more likely to encounter graph flaws by Voronoi Diagram [26], [27], [28].

Definition 4. (Voronoi Diagram [26], [27], [28]) Given a dataset D consisting of points in \mathbb{R}^d with d -dimensional real numbers, the Voronoi cell of any point $x_g \in D$ is represented as $V_D(x_g) = \{x \in \mathbb{R}^d, \text{dis}(x_g, x) \leq \text{dis}(x_b, x), \forall x_b \in D\}$, where each point x_g is noted as a Voronoi site. The set of all Voronoi cells of D is its Voronoi diagram $Vor(D)$.

According to this definition, each Voronoi cell $V_D(x_g)$ is a subspace in \mathbb{R}^d . Any point that lies within the subspace have x_g as its closest Voronoi site. It means that for any query within this cell, its nearest neighbor should be the point x_g .

We consider each base point x_b in the dataset D as a Voronoi site. In a high-dimensional space, each base point and its k -NNs are likely to be *locally homogeneous* [29]. This means that the cells where the k -NNs are uniformly distributed in various directions of the cell $V_D(x_b)$. Additionally, for most k -NNs of x_b , their corresponding cells are adjacent to the cell $V_D(x_b)$.

Heuristic. We use a heuristic to generate query points to detect flaws: *points near the boundary between two adjacent Voronoi cells are more likely to encounter flaws*. It's because these points have similar distances to the two Voronoi sites, making it easier to deviate from the optimal path during the search

process and enter another cell. The base point is guaranteed to be adjacent to the two cells belonging to its nearest neighbor. The k -NNs with larger rankings (i.e., larger k) may fail to meet the homogeneity requirement.

Approximation. To address this problem, our simple approximation is to only consider the k -NNs with smaller ranks (i.e., smaller k) for point generation. Simultaneously, this approach avoids comparing with distant neighbors. Under the widely used edge pruning strategies [20], [7], there's a high probability to prune the longest edge in any triangle. Thus, in the original proximity graph, the distant neighbors will not have an edge connected to the base point.

Given the base point x_b and its nearest neighbor point $x_k \in NN_k(x_b)$, the generated query point is:

$$x_e = \omega \cdot x_b + (1 - \omega) \cdot x_k \quad (1)$$

where ω is a parameter used to control the distance between the generated query point and the base point.

As shown in Figure 6, the generated query point lies near the perpendicular bisector of the line connecting two base points. To ensure that $x_e \notin V_D(x_k)$, we control $\omega > 0.5$. In most cases (i.e., when the two cells are adjacent), we can ensure that $x_e \in V_D(x_b)$. In other words, given the base point x_b , we can generate its corresponding error-prone points based on its k -NNs. Further, by searching on the graph, we can obtain a self-generated search logs to enhance the recall for all queries whose global optimum is the given base point.

V. LOG-BASED SEARCH ENHANCEMENT

A. Optimization on the Nearest Neighbor Search

According to Theorem IV.1 and Observations 1-3, we can infer that local optima are likely to be among the k -NNs of a base point. We can then group queries based on the local optima they converge to. Since the number of queries greatly exceeds k , many queries will converge to the same local optimum. This suggests that the routing edge from the local optimum to the global optimum is missing. To address this, we can construct a conjugate graph with edges connecting local optima to their corresponding global optima. After the first-stage search concludes, the conjugate graph directs all queries that converged to local optima towards the global optimum.

We use two categories of search logs: the self-generated search logs and the historical search logs. Following Theorem IV.1 and Observations 1-3, we generate queries for each base node to identify potential flaws. Then, the historical search logs are used to complement queries that their local optima do not belong to their k -NNs. Note that, the global optima of the search log can be obtained through both user complaints and asynchronous computations [30], [31]. For example, in facial recognition payment systems [32], [33], a failure query may require the user to provide additional information, such as a phone number, to complete the payment process. In our approach, we assume that the full search log is collected.

As shown in Algorithm 3, the first step is to add the historical search log to the experience set E (Lines 1-2). The experience set is used to record specific local optima found by greedy

Algorithm 3: Conjugate Graph Update

Input: proximity graph G , conjugate graph G' , initial nodes I , search parameters L_2, k , generate parameter ω, k_g, m
Output: Updated Conjugate Graph G'

```
1 initialize  $E$  as an empty set
2  $E \leftarrow$  historical search result  $\{x_l, x_g\}$  with parameter  $L_2$ 
3 foreach  $x_b \in G$  do
4    $ANN_k(x_b) \leftarrow$  approximate  $k_g$ -NNs
5   foreach  $x_k \in ANN_k(x_b)$  do
6      $x_e \leftarrow \omega \cdot x_b + (1 - \omega) \cdot x_k$ 
7      $x_l \leftarrow \text{GreedySearch}(G, I, x_e, L_2, k)$ 
8      $x_g \leftarrow \arg \min_{x \in ANN_k(x_b) \cup \{x_b\}} \text{dis}(x, x_e)$ 
9     if  $x_l \neq x_g$  then
10       $E \leftarrow E \cup \{x_l, x_g\}$ 
11 foreach  $\{x_l, x_g\} \in E$  do
12    $\_ \leftarrow$  insert edge  $(x_l, x_g)$  in  $G'$ 
13 return  $G'$ 
```

search with parameter L_2 and their corresponding global optima. Note that we emphasized L_2 , which is the search parameters of the log that converge to the local optimum. When the query is performed, the best enhancement with conjugate graph can be achieved only when search parameter $L = L_2$. When $L \neq L_2$, the search process may converge to a different local optimum. Thus, the routing edges in conjugate graph cannot be utilized. We also discussed experimentally how the different L values can affect performance in Appendix VI-C.

Then, we use the self-generated method in Appendix IV-B to obtain more local optima. Firstly, we choose to generate queries using k_g -NNs of each base point, where k_g is the parameter to adjust the number of generated queries. Since we can hardly search the accurate k_g -NNs for each base node, we use the approximate k_g -NNs as replacement (Lines 4-5). It can be quickly obtained by using the construction log stored in the conjugate graph, which we will discuss in Algorithm 4. For each neighbor in k_g -NNs, we generate a query point x_e with Equation 1 (Line 6).

After generating queries, we perform a greedy search to obtain potential local optimum (Line 7). Since $x_e \in V_D(x_b)$ and $V_D(x_b)$ is surrounded by the Voronoi cell of its k -NNs, we can quickly obtain an approximate global optimum from these cells (Line 8). Then, we add self-generated search logs to the experience set E (Lines 7-10). Finally, each element in the experience set E is treated as a directed edge and added to the conjugate graph G' (Lines 11-12). We have the following theorem to guarantee the accuracy of the nearest neighbor search with our EnhanceGraph framework:

Note that, Algorithm 3 is an approximation based on Opportunity 1. In fact, a small value of k_g is sufficient to achieve higher $\text{Recall}@1$. This is because Opportunity 1 states

Algorithm 4: Proximity and Conjugate Graph Construction

Input: proximity graph G , conjugate graph G' initial nodes I , search parameters L_1, k , maximum degree r
Output: Proximity Graph G , Conjugate Graph G'

```
// Phase 1: construct proximity graph
1 foreach  $x_b \in G$  do
2    $R, V_b \leftarrow \text{GreedySearch}(G, I, x_b, L_1, k)$ 
3    $N_b \leftarrow \text{Prune}(V_b, r)$ 
4   foreach  $x_n \in N_b$  do
5     add edges between  $x_b$  and  $x_n$  in  $G$ 
6     if  $|G[x_n]| > r$  then
7        $G[x_n] \leftarrow \text{Prune}(G[x_n], r)$ 
8    $G'[x_b] \leftarrow R$ 
/* Phase 2: construct conjugate graph */
9 foreach  $x_b \in G$  do
10   $G'[x_b] \leftarrow G'[x_b] - G[x_b]$ 
11 return  $G, G'$ 
```

that the local optimum found by the query is likely to be in the k -NNs of the global optimum in a high probability. In other words, it is highly probable that $x_l \in NN_k(x_g)$ for the added edges (x_l, x_g) . Furthermore, since k_g is small, the number of added edges is also small. Let M be the maximum rank of the local optimum in the $NN_k(x_g)$. Then, the size of added edges is bounded by $O(Mn)$, where n is the number of base points.

Discussion. When recall is high, improving it with traditional graph-based index optimization becomes difficult. A key advantage of our EnhanceGraph is that it can detect and fix the flaws of the current indexes, then continuously improve their recall even when it is high, without sacrificing search efficiency. It's because we only access the conjugate graph at the end of the search on proximity graph. At most, the neighbors of two additional nodes are computed (global optimum and local optimum, respectively). The resulting QPS reduction is equivalent to increasing the search parameter L by 2.

B. Optimization on k -NNs Search

The k -NNs graph can guarantee $\text{Recall}@1$ as it's a Monotonic Search Network (MSNET) [7] (i.e., it can always find a monotonic decreasing path between any two base points). It can also guarantee $\text{Recall}@k$ by fully connecting each base point with its nearest neighbors. However, the short edges making forward steps during the greedy search in Algorithm 1 are also short on a k -NNs graph. In other words, the minimal distance between the query and points in the candidate set decreases slowly, resulting in a large number of iterations in the greedy search. Additionally, due to the high degree of each node, more points need to be explored in each iteration. They

both increase the search overhead due to additional distance computations.

Some existing graph-based indexes [23], [7], [9] approximate RNG or MRNG by adopting the same edge pruning strategies to remove redundant edges. They strive to carefully select edges in the graph indexes to reduce the number of iterations and shrink the fan out of each iteration. They use incremental insertion for construction, similar to the Algorithm 4. Initially, a greedy search is performed for each newly inserted point (Lines 1-2), as shown in Algorithm 1. Then, for the visited list V , redundant edges are eliminated based on a specific edge pruning strategy (Line 3). For example, the pruning strategies prune the longest edges of all possible triangles (RNG [20] strategy), or ensure that the angle between any two edges is greater than 60 degrees (MRNG [7] strategy). Finally, the remaining edges are inserted into the graph (Lines 4-7).

During the construction process, approximate k -NNs are found for each base point (Line 2). However, this construction log is not further utilized. Only the pruned set of edges N_b is kept for insertion into the proximity graph (Phase 1). The pruned edges may reduce the navigation efficiency, but they are valuable as non-routing edges. We store them in the conjugate graph G' (Line 8). Finally, we remove redundant edges that already exist in the proximity graph to improve storage efficiency (Lines 9-10).

We use $ANN_k(x_b) = G[x_b] \cup G'[x_b]$ as an approximate k -NNs, which has two usages in our framework. First, during generating error-prone points, we use $ANN_k(x_b)$ as the approximate k -NNs. Second, improve $Recall@k$ when $Recall@1$ is close to 100%. As mentioned before, we can assume that there is a large overlap of the k -NNs between the query and its corresponding global optimum. Therefore, once we have ensured a high probability of finding the global optimum, we can complement the search results with its neighbors in the conjugate graph.

Discussion. Note that, unlike traditional indexes for table data, in-memory indexes [7], [9], [24] for vectors need to load all vectors into memory for DCO (Distance Comparison Operation). Disk-based indexes [23], [12] also require significant IO operations to load vectors from the disk. The memory footprint of the graph structure is typically much smaller than that of vectors. For example, the memory footprint of a graph index with a maximum degree of 32 is approximately equivalent to adding 32 extra dimensions to each vector. However, for many applications, such as RAG (Retrieval Augmented Generation) [34], the dimension of vectors is large (e.g., the latest embedding model used by OpenAI uses vectors with a dimension of 1536 [35]). Thus, the extra memory footprint of conjugate graph is also acceptable even when memory is limited.

VI. EXPERIMENTAL STUDY

A. Experiment Setups

Datasets. We use seven real-world public datasets that are widely adopted by ANN Benchmarks [36] and existing stud-

TABLE I: Datasets.

| Dataset | Dimension | #Base | #Query | Metric |
|--------------|-----------|-------|--------|---------------|
| GIST1M | 960 | 1000K | 1K | Euclidean |
| MNIST | 784 | 60K | 10K | Euclidean |
| Fasion-MNIST | 784 | 60K | 10K | Euclidean |
| FACE | 256 | 800K | 800K | Inner Product |
| GloVe-200 | 200 | 1183K | 10K | Angular |
| SIFT1M | 128 | 1000K | 10K | Euclidean |
| GloVe-100 | 100 | 1183K | 10K | Angular |
| DEEP1B | 96 | 9990K | 10K | Angular |

TABLE II: Experimental Settings.

| Parameters | Values |
|--|----------------------------------|
| Proximity graph construction parameter L_1 | 20, 40, 60, 80, 100 |
| Conjugate graph update parameter L_2 | 20, 40, 60, 80, 100 |
| Position parameter of generated queries ω | 0.51 , 0.6, 0.7, 0.8, 0.9 |
| Number of generated queries k_g per base node | 5 |

ies [23], [9], [7], [24]. To demonstrate the effectiveness of our approach, we also use an anonymous industrial dataset called FACE. The main characteristics of datasets are summarized in Table I. *Dimension* is the vector dimension. *#Base* refers to the number of base points, which are used to construct the graph index. *#Query* is the number of queries used to evaluate the performance of algorithms. *Metric* is the distance computation function. Note that the data size is also widely adopted in many in-memory index studies [17], [9], [7], [24]. In practice, disk-based indexes [23], [12] are commonly used to handle larger datasets.

Compared Algorithms. We integrate EnhanceGraph in four state-of-the-art graph-based indexes:

- *NSG* [7]: It is built using the MRNG [7] strategy for edge pruning.
- *VAMANA*. [23]: It is built based on MRNG strategy. It uses more slack pruning criteria compared to MRNG and a random graph for initialization.
- τ -*MNG* [24]: It uses a proximity graph for initialization. Its edge pruning strategy includes all edges with a distance less than 3τ . It keeps long edges that are sufficiently long for navigation.
- *HNSW*. [9]: It is constructed hierarchically using the RNG [20] edge pruning strategy. The bottom layer serves as the complete proximity graph. The higher layer samples a subset of points to construct the graph, which acts as a highway in search process.

The conjugate graph proposed in this paper can be applied to any graph indexing. We use the algorithm name appending “-SC” to indicate that both Search and Construction logs are used to construct the conjugate graph (e.g., VAMANA-SC).

Environment. All experiments are implemented in C++ and compiled with -Ofast optimization. The experiments on public datasets are conducted on a single server equipped with a Intel(R) Xeon(R) Gold 6258R CPU@2.70GHz with 28 CPU cores and 1024 GB RAM. The experiments on FACE dataset are conducted on a single server equipped with a Intel(R) Xeon(R) Platinum 8163 CPU@2.50GHz with 96 CPU cores and 512GB RAM.

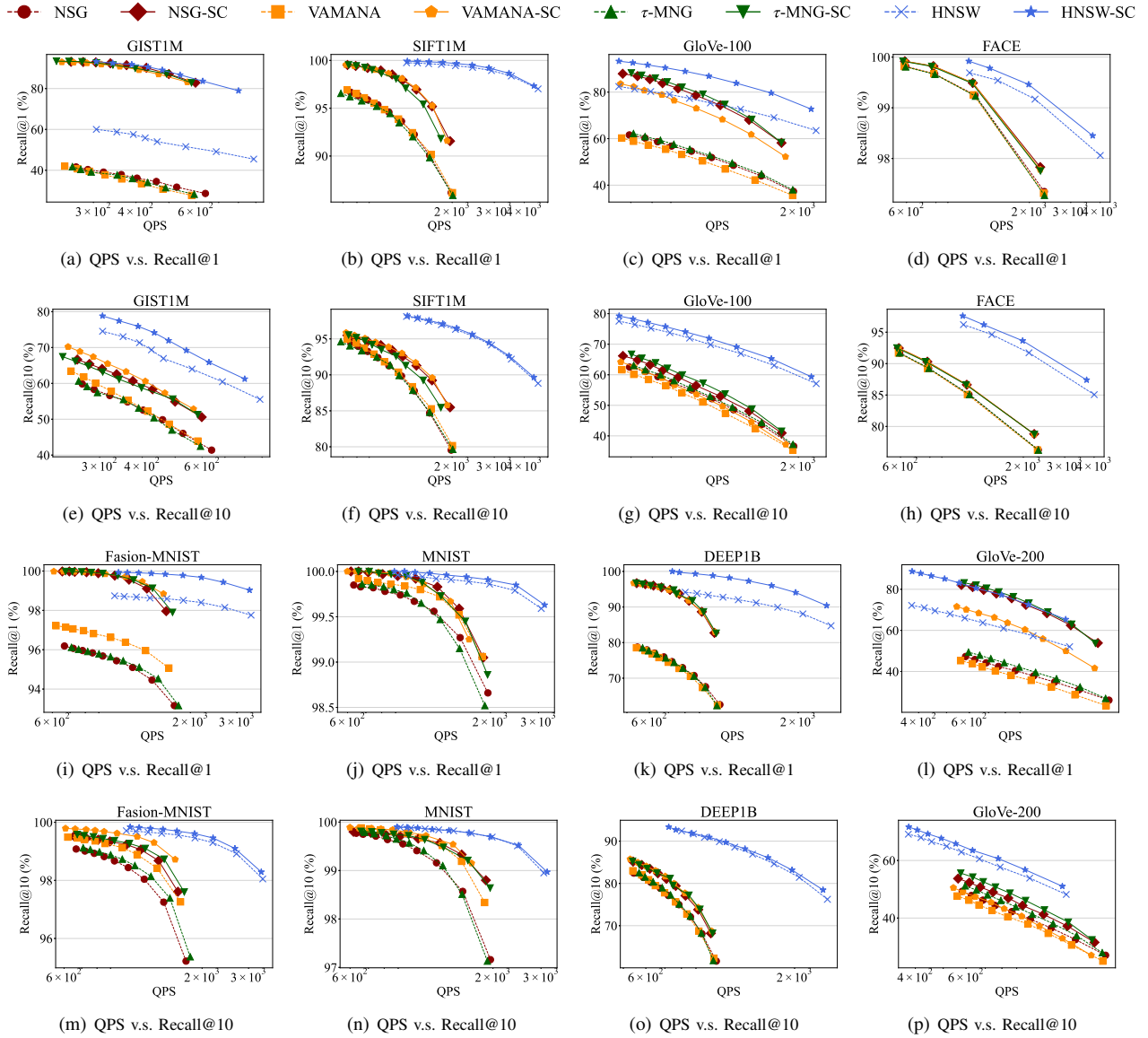


Fig. 7: Time-Accuracy Tradeoff (Varying Algorithms).

Measurements. We use the recall rate [7], [23], [9] (i.e., the ratio of searched nearest neighbors to the accurate nearest neighbors) to measure the accuracy of the algorithm. Here, $Recall@k$ is the recall of the k -NNs. We use query-per-second (QPS), the number of requests that can be processed in each second, to measure efficiency. We measure the in-memory index, so the vectors data also needs to be loaded into memory. Thus, *Memory Usage* is the total size of the vectors data and the graph index. The *Build Time* is the time taken to construct the graph index and update the conjugate graph.

Implementation. As there are a few query points in public datasets, we generate one historical search point. Specifically, we calculate the mean of the absolute value of each dimension of the base points, denoted by η . Then, we add random noise sampled from a uniform distribution $U(-0.5\eta, 0.5\eta)$ to each dimension of the base points to generate the historical search points. The random noise is extensively utilized in computer

vision and other learning fields [37], [38]. The test query points are also sampled from the distribution with guarantee that there is no test queries existing in the historical search queries. We then use the two types of search logs to update the conjugate graph. For the FACE dataset, we only use four real historical queries for each base point to update the conjugate graph. The original index is constructed through incremental inserts on a single core, due to data dependencies between insertions. The update of the conjugate graph runs on 28 cores using the OpenMP library. Besides, we used AVX2 SIMD libraries for optimizing the distance computation. In addition, our EnhanceGraph algorithm has been integrated into Ant Group's open-source vector library, VSAG².

Parameters. We set the maximum degree of the graph $r = 12$ to demonstrate the effectiveness of our algorithm, which is

²VSAG: <https://github.com/antgroup/vsag>

TABLE III: Comparison of Enhancement, Memory Usage and Build Time. (Fixed Search Parameter)

| Algorithm | GIST1M (Vector Data Size: 3662.11MB) | | | | | GloVe-200 (Vector Data Size: 902.95MB) | | | | |
|----------------|--------------------------------------|---------------|---------------|------------------|--------------|--|---------------|---------------|-----------------|--------------|
| | QPS | Recall@1 | Recall@10 | Memory Usage | Build Time | QPS | Recall@1 | Recall@10 | Memory Usage | Build Time |
| NSG | 267.3 | 41.61% | 59.83% | 3688.46MB | 2902s | 555.7 | 47.29% | 49.29% | 949.92MB | 2332s |
| NSG-SC | 260.0 | 93.12% | 66.65% | 3737.43MB | 3604s | 549.8 | 82.09% | 53.70% | 1002.23MB | 2866s |
| VAMANA | 246.0 | 42.01% | 63.41% | 3705.16MB | 3757s | 546.4 | 45.26% | 47.65% | 958.54MB | 2688s |
| VAMANA-SC | 244.4 | 92.98% | 70.21% | 3750.02MB | 4322s | 522.7 | 82.10% | 52.17% | 1010.3MB | 3191s |
| τ -MNG | 267.4 | 41.74% | 60.64% | 3693.93MB | 3029s | 535.6 | 49.37% | 51.18% | 964.19MB | 2402s |
| τ -MNG-SC | 260.4 | 93.42% | 67.44% | 3738.25MB | 3448s | 519.6 | 83.14% | 55.60% | 1009.29MB | 2838s |
| KNNG | 306.1 | 49.41% | 52.29% | 3802.11MB | 16483s | 360.8 | 67.25% | 64.70% | 1070.37MB | 13512s |
| HNSW | 327.4 | 60.01% | 74.52% | 3773.46MB | 2944s | 388.1 | 72.17% | 69.12% | 1034.73MB | 2913s |
| HNSW-SC | 322.7 | 93.24% | 78.81% | 3817.11MB | 3420s | 380.7 | 88.68% | 71.64% | 1081.92MB | 3190s |

commonly used in existing studies [9]. The maximum degree of the graph is set to $r = 32$ in the experiment varying parameters L_1 , L_2 , and ω . As demonstrated in Table II, we adjust three major parameters at different values to examine their influence on the conjugate graph enhancement. We fix $k_g = 5$ to generate k_g search queries for each base point to obtain self-generated search log.

B. Overall Results

Overall Results (Time-Accuracy Trade-Off). As shown in Figure 7, we examine the Time-Accuracy Tradeoff of four algorithms on each dataset. The dashed lines in various colors represent different proximity graphs, while the solid lines represent the version that utilized a conjugate graph to enhance (i.e., our EnhanceGraph framework). We found that the conjugate graph boosts the recall rate for each algorithm at the same QPS. In GIST1M, it enhances *Recall@1* the most from 41.74% to 93.42%.

The improvement is mainly due to the substantial number of edges added from the search log in the conjugate graph. These edges help the search process efficiently move from local optima to global optima. Especially on the FACE dataset, our EnhanceGraph framework improves the recall, even when it's already high (i.e., it improves *Recall@1* from 99.8% to 99.9%). However, for some low dimension datasets (e.g. SIFT1M), conjugate graph may hardly improve the recall since it's already high (e.g., more than 99%). Besides, the conjugate graph improves *Recall@10*. The improvement is attributed to the use of construction log, which preserves numerous pruned k -NNs in the proximity graph.

Overall Results (Memory Usage and Build Time).

As shown in Table III, we evaluated the enhancement on GIST1M and GloVe-200 datasets. The conjugate graph is constructed using both search and construction logs across four graph structures. As a comparison of extra space and enhancement, we constructed a KNNG (k -NNs Graph) without using the pruning strategy and set the maximum degree to $r = 36$. The search list length of algorithms, except for KNNG, was set at $L = 100$. We found that NSG-SC, τ -MNG-SC, and VAMANA-SC all significant improve the *Recall@1* from 41.74% to 93.42% on GIST1M. On the GloVe-200 dataset, the conjugate graph increases *Recall@1* to over 80%. There's no obvious decrease in QPS during this process, because we use the conjugate graph only as the last supplementary step after searching on the proximate graph. Figure 7 also shows

that our algorithms outperform the baselines when fixing the same QPS.

The extra space cost of constructing the conjugate graph stabilizes across datasets. This is primarily because the size of the conjugate graph mainly depends on the maximum degree r , which is a constant in our experimental setup. Although the size of the conjugate graph is comparable to the proximity graph, both are relatively small compared to the size of the data. For instance, a 50MB conjugate graph is still relative small compared to a 3662.11MB dataset. Among them, the memory usage of KNNG is larger than that of all algorithms except HNSW-SC.

C. Evaluation on Varying Parameters

Results of Varying Generate Parameter ω . As shown in Figure 10, we demonstrate the effect of updating the conjugate graph using points generated with different parameters ω . As before, different colors correspond to different parameters. Solid lines represent the use of the conjugate graph, while dashed lines represent its absence. For the simple dataset, GloVe-200, the ω setting has less impact on the final performance. However, for the more challenging dataset GIST1M, a smaller ω setting allows the conjugate graph to improve recall more significantly. This further confirms that a smaller ω generates query points that are more likely to identify flaws in the proximity graph, and then fix and refine the indexes.

Results of Varying Construction Parameter L_1 . As shown in Figure 8, we demonstrate the improvement brought by the conjugate graph when we construct VAMANA with a different construction parameter L_1 . As L_1 increases, we see a significant enhancement in using only the proximity graph search, as depicted by the dotted line. This is because a larger L_1 leads to superior graph quality. Consequently, the conjugate graphs constructed using construction log also possess higher quality. In other words, the union of the conjugate graph and the proximity graph is more similar to an accurate k -NNs graph. This leads to the most substantial improvement on *Recall@10*.

Results of Varying Update Parameter L_2 . As shown in Figure 9, we examine the impact of different parameters L_2 on the updating conjugate graph. We discover that when $L_2 < 100$, a significant turning point appears on the curve at a specific point, precisely when the search parameter $L = L_2$. This is because we have set the maximum search size to $L = 100$. When $L > L_2$, the recall rate drops as QPS decreases, which corresponds to an increase in L . This happens because we

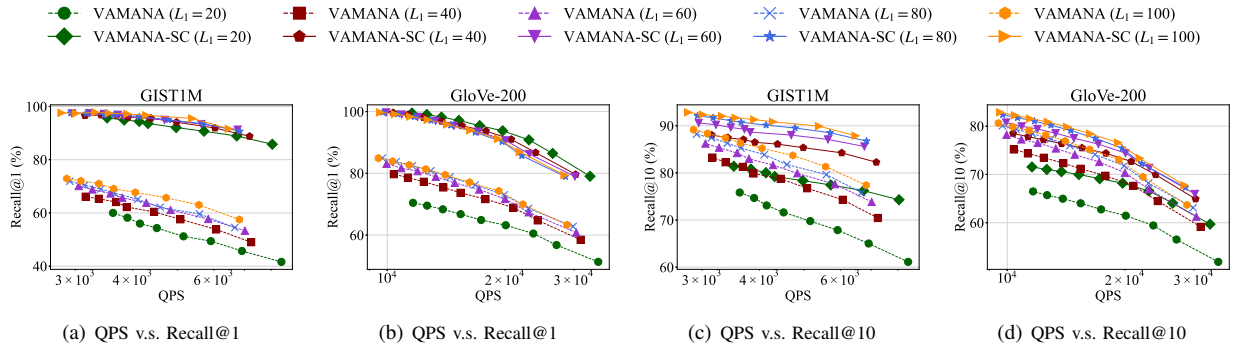


Fig. 8: Time-Accuracy Trade-off (Varying L_1).

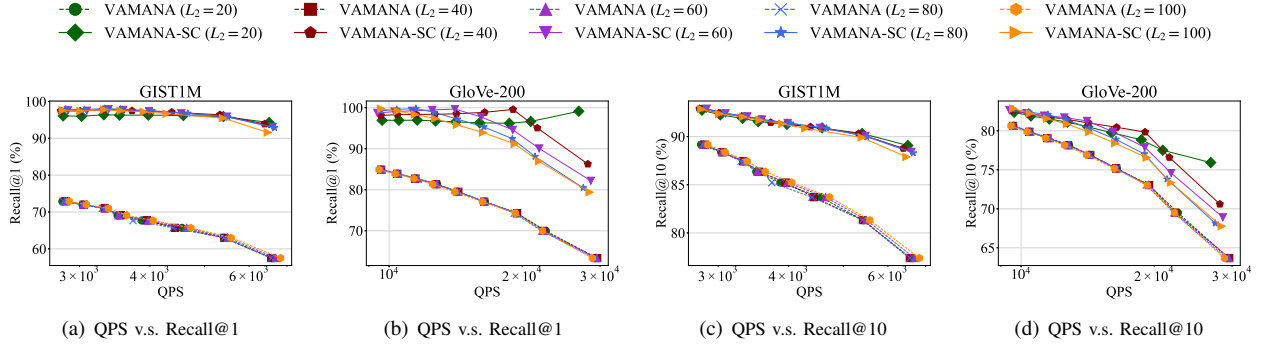


Fig. 9: Time-Accuracy Trade-off (Varying L_2).

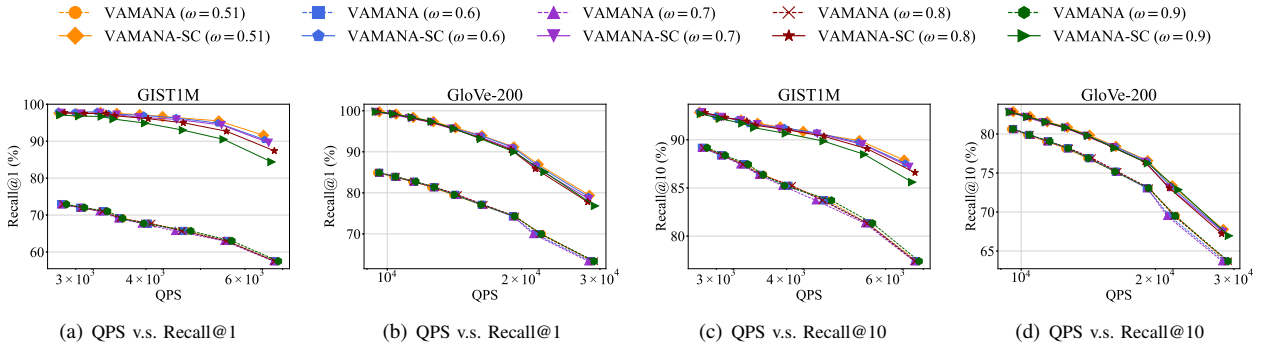


Fig. 10: Time-Accuracy Trade-off (Varying ω).

only utilize the local optimum that is reached when searching for the list size $L = L_2$ to connect to the global optimum. For $L > L_2$, there's a high possibility that the search process converges to a better local optimum, which might not have an edge connected to the global optimum. Thus, this affects the improvements brought about by the conjugate graph. However, this provides a new insight: our method can approach the optimization cap even with a small search parameters L .

Results of Shot Rate (Varying Generate Parameter ω). As shown in Figure 11, we generate query points by adjusting parameters ω near the middle vertical line of each base point and base point's nearest neighbor. We then search for the local optimum of these query points. We evaluated the result of VAMANA and HNSW on GIST1M and GLoVe-100. The blue bars indicate the rate of reaching the global optimum,

while the orange bars represent the rate at which the local optimum is the base point's nearest neighbor. The green bars show the rate at which the local optimum is the other point. We find that the local optimum is either the base point or the base point's nearest neighbor in over 95% of the points in VAMANA. Many points near the middle vertical line struggle to reach the global optimum (i.e., corresponding base point).

As ω increases, more points reach the global optimum in search process. Most points that don't reach the global optimum in VAMANA end up reaching the nearest neighbor of global optimum. This results in a significant number of edges we connect in the conjugate graph are from the global optimum's nearest neighbor to the global optimum, implying that the number of local optimum is finite. On the other hand, the search process converges to another point in HNSW more

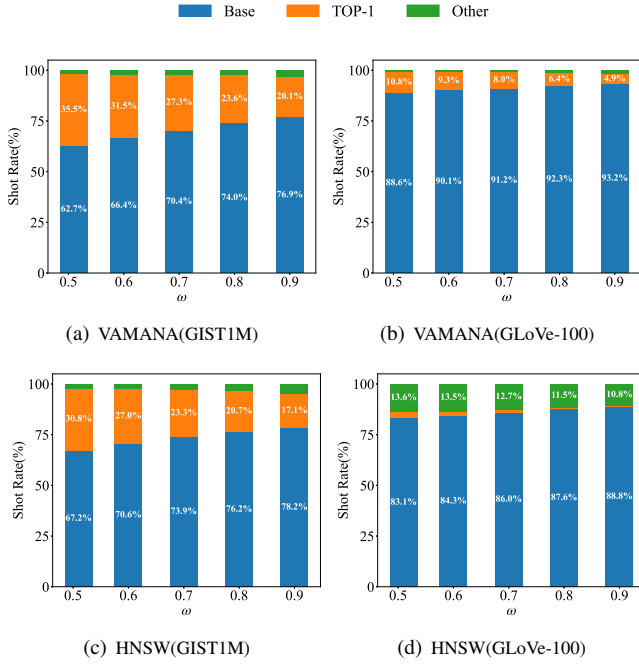


Fig. 11: Shot Rate on Different Queries (Varying ω)

frequently than in VAMANA, due to the increased uncertainty in the search process caused by the hierarchical structure of HNSW. It's because HNSW chooses different starting points in the bottom graph for each query, leading to varied convergence results.

Summary of the Experimental Results:

- EnhanceGraph can significantly improve *Recall@1*, with the most improvement increasing from 41.74% to 93.42% on GIST1M.
- EnhanceGraph can improve *Recall@10* without sacrificing searching efficiency.
- EnhanceGraph can achieve the optimal performance with acceptable additional memory usage and build time.

VII. RELATED WORK

Graph-based indexes. The Relative Neighborhood Graph (RNG) [20] and Sparse Neighborhood Graph (SNG) [39] approximate the k -NNs graph and add shortcuts by using specific edge pruning strategy. The Diversified Proximity Graph (DPG) [21] is based on the RNG, which ensures that the edges are evenly distributed over the angle. However, the edge pruning strategy of RNG is too tight to make it sufficient to be a MSNET [7]. The Monotonic Relative Neighborhood Graph (MRNG) [7] uses a looser strategy so that more edges can be reserved for navigation. It ensures that there exists a Monotonic Decrease Path [7] from any source node to any target node.

Constructing a theoretical graph structure like whether RNG or MRNG incurs high cost. Therefore, in engineering, many graphs approximate them to achieve a lower construction cost. The Navigating Spreading-out Graph (NSG) [7] use the edge pruning strategy of MRNG and limit the property of MSNET with searching start from a fixed node. Subramanya *et al.*

proposed Vamana [23], [8], [40] as an approximation of NSG, which further loose the strategy. τ -MG [24], on the other hand, is optimized based on MRNG. It specifies that the short edges should be short enough and the long edges should be long enough. HNSW [9] is a hierarchical graph index constructed based on multiple layers of graph. However, these graph indexes remain static after construction. Then, some query vectors and other similar query vectors converge to the same local optimum, and the global optimum is never found. At the lowest level, it is a complete NSW, while the higher levels facilitate quick location of the highway near the query point during search.

Partition-based indexes. Nowadays, there are various methods for dividing the data space into subspaces with specific properties. For instance, vectors within a subspace are relatively close to each other, allowing for high-performance searching within that subspace. Tree-based methods like QD-tree [41], [3], [42] and KD-tree [43], [11], [44] create a hierarchical structure, with each leaf node representing a subspace and internal nodes containing collections of subspaces. Hash-based methods, like LSH [13], [45], [15], utilize locally sensitive hashing to assign similar points to the same buckets while ensuring balanced bucket sizes. Another commonly used method is IVF [46], which is similar to LSH but uses clustering to partition the buckets. However, ensuring search recall for boundary points requires searching across a large number of clusters simultaneously, further increasing the search cost. Additionally, the Curse of Dimensionality [47], [4] occurs when the dimension of points increases. It becomes challenging to utilize similarity information within delineated subspaces, resulting in poor search performance.

Compression-based indexes. Computation for the distance of high dimensional data is a significant bottleneck for most existing methods. Recent studies focus on compressing the original high dimensional data into a lower-dimensional space to reduce the time-consuming distance computation. One common compression method for distance preservation is Product Quantization (PQ) [48], [49]. It clusters vector segments and maps them to the IDs of cluster centers. This allows for quick approximate distance computation using pre-computed center-to-center distances. ADsampling [25] combines the stochastic mapping and early stop to propose a fast distance comparison strategy that can provide correct results with high probability.

VIII. CONCLUSION

In this paper, we address the issue that construction and search logs have not been well utilized in existing graph-based indexes for ANNS. We introduce EnhanceGraph, a novel framework designed to continuously refine graph-based indexes. It assimilates information of construction and search logs into a single, cohesive conjugate graph. As search queries are completed within the proximity graph, the conjugate graph intervenes to enhance the findings by pinpointing potential global optimum and supplementing the missing k -NNs. Leveraging this novel approach, we substantially increase *Recall@1* from 41.74% to 93.42% without sacrificing efficiency.

REFERENCES

- [1] P. Grother, M. Ngan, and K. Hanaoka, “Ongoing face recognition vendor test (frvt) part 2: Identification,” 2018-11-27 2018.
- [2] J. Suchal and P. Návrat, “Full text search engine as scalable k-nearest neighbor recommendation system,” in *Artificial Intelligence in Theory and Practice III* (M. Bramer, ed.), (Berlin, Heidelberg), pp. 165–173, Springer Berlin Heidelberg, 2010.
- [3] J. Mohoney, A. Pacaci, S. R. Chowdhury, A. Mousavi, I. F. Ilyas, U. F. Minhas, J. Pound, and T. Rekatsinas, “High-throughput vector similarity search in knowledge graphs,” *Proc. ACM Manag. Data*, vol. 1, jun 2023.
- [4] M. Verleysen and D. François, “The curse of dimensionality in data mining and time series prediction,” in *International work-conference on artificial neural networks*, pp. 758–770, Springer, 2005.
- [5] P. Indyk and R. Motwani, “Approximate nearest neighbors: towards removing the curse of dimensionality,” in *Proceedings of the thirtieth annual ACM symposium on Theory of computing*, pp. 604–613, 1998.
- [6] B. Harwood and T. Drummond, “Fanng: Fast approximate nearest neighbour graphs,” in *Proceedings of the IEEE Conference on Computer Vision and Pattern Recognition (CVPR)*, June 2016.
- [7] C. Fu, C. Xiang, C. Wang, and D. Cai, “Fast approximate nearest neighbor search with the navigating spreading-out graph,” *Proc. VLDB Endow.*, vol. 12, p. 461–474, jan 2019.
- [8] S. Gollapudi, N. Karia, V. Sivashankar, R. Krishnaswamy, N. Begwani, S. Raz, Y. Lin, Y. Zhang, N. Mahapatro, P. Srinivasan, A. Singh, and H. V. Simhadri, “Filtered-diskann: Graph algorithms for approximate nearest neighbor search with filters,” in *Proceedings of the ACM Web Conference 2023*, WWW ’23, (New York, NY, USA), p. 3406–3416, Association for Computing Machinery, 2023.
- [9] Y. A. Malkov and D. A. Yashunin, “Efficient and robust approximate nearest neighbor search using hierarchical navigable small world graphs,” *IEEE Transactions on Pattern Analysis and Machine Intelligence*, vol. 42, no. 4, pp. 824–836, 2020.
- [10] S. Arya, D. M. Mount, N. S. Netanyahu, R. Silverman, and A. Y. Wu, “An optimal algorithm for approximate nearest neighbor searching fixed dimensions,” *Journal of the ACM (JACM)*, vol. 45, no. 6, pp. 891–923, 1998.
- [11] P. Ram and K. Sinha, “Revisiting kd-tree for nearest neighbor search,” in *Proceedings of the 25th ACM SIGKDD International Conference on Knowledge Discovery & Data Mining, KDD ’19*, (New York, NY, USA), p. 1378–1388, Association for Computing Machinery, 2019.
- [12] Q. Chen, B. Zhao, H. Wang, M. Li, C. Liu, Z. Li, M. Yang, and J. Wang, “Spann: Highly-efficient billion-scale approximate nearest neighborhood search,” in *Advances in Neural Information Processing Systems* (M. Ranzato, A. Beygelzimer, Y. Dauphin, P. Liang, and J. W. Vaughan, eds.), vol. 34, pp. 5199–5212, Curran Associates, Inc., 2021.
- [13] Q. Lv, W. Josephson, Z. Wang, M. Charikar, and K. Li, “Multi-probe lsh: efficient indexing for high-dimensional similarity search,” in *Proceedings of the 33rd international conference on Very large data bases*, pp. 950–961, 2007.
- [14] J. Li, X. Yan, J. Zhang, A. Xu, J. Cheng, J. Liu, K. K. W. Ng, and T.-c. Cheng, “A general and efficient querying method for learning to hash,” in *Proceedings of the 2018 International Conference on Management of Data, SIGMOD ’18*, (New York, NY, USA), p. 1333–1347, Association for Computing Machinery, 2018.
- [15] X. Zhao, Y. Tian, K. Huang, B. Zheng, and X. Zhou, “Towards efficient index construction and approximate nearest neighbor search in high-dimensional spaces,” *Proceedings of the VLDB Endowment*, vol. 16, no. 8, pp. 1979–1991, 2023.
- [16] W. Li, Y. Zhang, Y. Sun, W. Wang, M. Li, W. Zhang, and X. Lin, “Approximate nearest neighbor search on high dimensional data—experiments, analyses, and improvement,” *IEEE Transactions on Knowledge and Data Engineering*, vol. 32, no. 8, pp. 1475–1488, 2019.
- [17] M. Wang, X. Xu, Q. Yue, and Y. Wang, “A comprehensive survey and experimental comparison of graph-based approximate nearest neighbor search,” *Proc. VLDB Endow.*, vol. 14, p. 1964–1978, jul 2021.
- [18] K. Hajebi, Y. Abbasi-Yadkori, H. Shahbazi, and H. Zhang, “Fast approximate nearest-neighbor search with k-nearest neighbor graph,” *IJCAI’11*, p. 1312–1317, AAAI Press, 2011.
- [19] Z. Jin, D. Zhang, Y. Hu, S. Lin, D. Cai, and X. He, “Fast and accurate hashing via iterative nearest neighbors expansion,” *IEEE Transactions on Cybernetics*, vol. 44, no. 11, pp. 2167–2177, 2014.
- [20] G. T. Toussaint, “The relative neighbourhood graph of a finite planar set,” *Pattern Recognition*, vol. 12, no. 4, pp. 261–268, 1980.
- [21] W. Li, Y. Zhang, Y. Sun, W. Wang, M. Li, W. Zhang, and X. Lin, “Approximate nearest neighbor search on high dimensional data — experiments, analyses, and improvement,” *IEEE Transactions on Knowledge and Data Engineering*, vol. 32, no. 8, pp. 1475–1488, 2020.
- [22] C. Fu, C. Wang, and D. Cai, “High dimensional similarity search with satellite system graph: Efficiency, scalability, and unindexed query compatibility,” *IEEE Transactions on Pattern Analysis and Machine Intelligence*, vol. 44, no. 8, pp. 4139–4150, 2022.
- [23] S. Jayaram Subramanya, F. Devvrit, H. V. Simhadri, R. Krishnaswamy, and R. Kadekodi, “Diskann: Fast accurate billion-point nearest neighbor search on a single node,” in *Advances in Neural Information Processing Systems* (H. Wallach, H. Larochelle, A. Beygelzimer, F. d’Alché-Buc, E. Fox, and R. Garnett, eds.), vol. 32, Curran Associates, Inc., 2019.
- [24] Y. Peng, B. Choi, T. N. Chan, J. Yang, and J. Xu, “Efficient approximate nearest neighbor search in multi-dimensional databases,” *Proceedings of the ACM on Management of Data*, vol. 1, no. 1, pp. 1–27, 2023.
- [25] J. Gao and C. Long, “High-dimensional approximate nearest neighbor search: with reliable and efficient distance comparison operations,” *Proc. ACM Manag. Data*, vol. 1, jun 2023.
- [26] S. Fortune, “Voronoi diagrams and delaunay triangulations,” in *Handbook of discrete and computational geometry*, pp. 705–721, Chapman and Hall/CRC, 2017.
- [27] D. Lee and B. Schachter, “Two algorithms for constructing a delaunay triangulation,” *International Journal of Parallel Programming*, vol. 9, pp. 219–242, 06 1980.
- [28] F. Aurenhammer, “Voronoi diagrams—a survey of a fundamental geometric data structure,” *ACM Comput. Surv.*, vol. 23, p. 345–405, sep 1991.
- [29] W. M. Goldman, “Locally homogeneous geometric manifolds,” in *Proceedings of the International Congress of Mathematicians 2010 (ICM 2010) (In 4 Volumes) Vol. I: Plenary Lectures and Ceremonies Vols. II–IV: Invited Lectures*, pp. 717–744, World Scientific, 2010.
- [30] W. Wu, L. Flokas, E. Wu, and J. Wang, “Complaint-driven training data debugging for query 2.0,” in *Proceedings of the 2020 ACM SIGMOD International Conference on Management of Data, SIGMOD ’20*, (New York, NY, USA), p. 1317–1334, Association for Computing Machinery, 2020.
- [31] P. W. Koh and P. Liang, “Understanding black-box predictions via influence functions,” in *International conference on machine learning*, pp. 1885–1894, PMLR, 2017.
- [32] L. Tang, “Revisiting facial-recognition payment: Old problems still lingering,” *Nielsen Norman Group*, vol. 20, 2022.
- [33] B. W. G. Lines, “No card, no phone, no problem! alipay: Pay with your face, a balance between convenience, security and privacy,” *Blog Writing Guide*, 2020.
- [34] P. Lewis, E. Perez, A. Piktus, F. Petroni, V. Karpukhin, N. Goyal, H. Küttler, M. Lewis, W.-t. Yih, T. Rocktäschel, et al., “Retrieval-augmented generation for knowledge-intensive nlp tasks,” *Advances in Neural Information Processing Systems*, vol. 33, pp. 9459–9474, 2020.
- [35] “[online] openai embedding docs.” <https://openai.xiniushu.com/docs/guides/embeddings>, 2024.
- [36] “[online] ann benchmarks.” <https://github.com/erikbern/ann-benchmarks>, 2024.
- [37] S. O. Rice, “Mathematical analysis of random noise,” *The Bell System Technical Journal*, vol. 23, no. 3, pp. 282–332, 1944.
- [38] A. Fawzi, S.-M. Moosavi-Dezfooli, and P. Frossard, “Robustness of classifiers: from adversarial to random noise,” in *Advances in Neural Information Processing Systems* (D. Lee, M. Sugiyama, U. Luxburg, I. Guyon, and R. Garnett, eds.), vol. 29, Curran Associates, Inc., 2016.
- [39] S. Arya and D. M. Mount, “Approximate nearest neighbor queries in fixed dimensions,” in *SODA*, vol. 93, pp. 271–280, 1993.
- [40] S. Jaiswal, R. Krishnaswamy, A. Garg, H. V. Simhadri, and S. Agrawal, “Ood-diskann: Efficient and scalable graph anns for out-of-distribution queries,” 2022.
- [41] Z. Yang, B. Chandramouli, C. Wang, J. Gehrke, Y. Li, U. F. Minhas, P.-r. Larson, D. Kossmann, and R. Acharya, “Qd-tree: Learning data layouts for big data analytics,” *SIGMOD ’20*, (New York, NY, USA), p. 193–208, Association for Computing Machinery, 2020.
- [42] X. Xie, S. Shi, H. Wang, and M. Li, “Sat: sampling acceleration tree for adaptive database repartition,” *World Wide Web*, vol. 26, no. 5, pp. 3503–3533, 2023.
- [43] K. He and J. Sun, “Computing nearest-neighbor fields via propagation-assisted kd-trees,” in *2012 IEEE Conference on Computer Vision and Pattern Recognition*, pp. 111–118, 2012.

- [44] R. Pinkham, S. Zeng, and Z. Zhang, "Quicknn: Memory and performance optimization of k-d tree based nearest neighbor search for 3d point clouds," in *2020 IEEE International Symposium on High Performance Computer Architecture (HPCA)*, pp. 180–192, 2020.
- [45] A. Andoni, P. Indyk, T. Laarhoven, I. Razenshteyn, and L. Schmidt, "Practical and optimal lsh for angular distance," *Advances in neural information processing systems*, vol. 28, 2015.
- [46] Y. Chen, T. Guan, and C. Wang, "Approximate nearest neighbor search by residual vector quantization," *Sensors*, vol. 10, no. 12, pp. 11259–11273, 2010.
- [47] M. Köppen, "The curse of dimensionality," in *5th online world conference on soft computing in industrial applications (WSC5)*, vol. 1, pp. 4–8, 2000.
- [48] H. Jegou, M. Douze, and C. Schmid, "Product quantization for nearest neighbor search," *IEEE transactions on pattern analysis and machine intelligence*, vol. 33, no. 1, pp. 117–128, 2010.
- [49] T. Ge, K. He, Q. Ke, and J. Sun, "Optimized product quantization for approximate nearest neighbor search," in *Proceedings of the IEEE conference on computer vision and pattern recognition*, pp. 2946–2953, 2013.